Climate Dynamics (2020) 55:2939–2956
https://doi.org/10.1007/s00382-020-05424-x

Summer and winter Atlantic Niño: connections with ENSO and implications

Aubains Hounsou-Gbo[1,2] · Jacques Servain[1,3] · Francisco das Chagas Vasconcelos Junior[1] · Eduardo Sávio P. R. Martins[1] · Moacyr Araújo[4,5]

Received: 19 February 2020 / Accepted: 18 August 2020 / Published online: 29 August 2020

Abstract

The teleconnection between the Atlantic Niño and the Pacific El Niño Southern Oscillation (ENSO) is revisited using observational and reanalysis data for the 1905–2014 period. Two types of Atlantic Niño are significantly negatively correlated with ENSO, with Atlantic leading ENSO by 6-month to 1-year. The first one is the already well-known connection between the boreal summer Atlantic Niño (ATL3: 3° N–3° S, 20° W–0°) and the subsequent winter ENSO (Niño3: 5° N–5° S, 150° W–90° W). This relationship is strong in the first and last decades of the study period. It is shown that a second Atlantic Niño in boreal fall/early winter (October–December, hereinafter called winter Atlantic Niño) is also significantly correlated with the following year ENSO. This winter Atlantic Niño leads to an early development of ENSO from boreal summer onwards, with a marked multidecadal modulation of the lead time. A nearly 1-year leading connection between winter Atlantic Niño and the following ENSO is generally observed in the mid-twentieth century, mostly when the summer Atlantic Niño teleconnection with the subsequent winter ENSO is weak. The same mechanism of the Atlantic–Pacific Niño connection, which involves the Walker circulation, operates for the two types of Atlantic Niño. Our analysis supports the leading influence of the summer and winter Atlantic equatorial modes on climate variability in South America. These results suggest the relevance of different types of Atlantic Niño for the 6-month to 1-year predictability of ENSO and its climatic impacts.

Keywords Atlantic equatorial mode · El Niño southern oscillation · Teleconnection · Predictability · South American climate

1 Introduction

The eastern equatorial Atlantic, a region dominated by the seasonal cycle, records its lowest annual sea surface temperature (SST) in summer[1] (Merle et al. 1980; Picaut 1983; Wauthy 1983; Caniaux et al. 2011). This seasonal cooling, which basically occurs during the local highest seasonal upwelling, results from the intensification of the southeastern trade winds in the late spring/early summer (Marin et al. 2009; Ding et al. 2009; Lubbëcke et al. 2018) when the intertropical convergence zone (ITCZ) is shifting to its northern position. Associated to the seasonal cold tongue development, the Atlantic equatorial mode (referred here and after as summer Atlantic Niño) is a dominant mode of interannual variability in the tropical Atlantic (Servain et al. 1982; Zebiak 1993; Marin et al. 2009; Lubbëcke et al. 2010). It is a coupled ocean–atmosphere mode like the El Niño-Southern Oscillation (ENSO) of the Pacific although with a

[1] All seasons indicated in this study are referred to boreal seasons.

✉ Aubains Hounsou-Gbo
h.aubains@gmail.com

[1] Research Institute for Meteorology and Water Resources (FUNCEME), Av. Rui Barbosa, 1246, Fortaleza, CE 60115-221, Brazil

[2] International Chair in Mathematical Physics and Applications (ICMPA-Unesco Chair), UAC, 072 P.O. Box 50, Cotonou, Benin

[3] Institut de Recherche pour le Développement (IRD), LOCEAN, Université de Paris 6, 75000 Paris, France

[4] Laboratório de Oceanografia Física Estuarina e Costeira (LOFEC), Department of Oceanography-DOCEAN, Federal University of Pernambuco-UFPE, Av. Arquitetura s/n, Recife, PE 50740-550, Brazil

[5] Brazilian Research Network on Global Climate Change (Rede CLIMA), Av. dos Astronautas, 1758, São José dos Campos, SP 1227-010, Brazil

smaller magnitude. Indeed, both Pacific and Atlantic Niños result from the Bjerknes positive feedback and peak in winter and summer respectively (Bjerknes 1969; Zebiak 1993; Keenlyside and Latif 2007). Although, in contrast to ENSO for which cold and warm events are asymmetric, Atlantic events are more spatially symmetric with similar Bjerknes feedback strength for warm and cold events (McPhaden and Zhang 2009; Lübbecke and McPhaden 2017). At multidecadal timescale, the variability of the summer Atlantic Niño is suggested to be enhanced during negative phases of the Atlantic multidecadal oscillation (AMO) (Martín-Rey et al. 2018).

Inside the same eastern equatorial Atlantic region, another seasonal SST cooling, much weaker than in the summer, occurs in early winter (Merle 1983). This second peak in November–December is associated with the second seasonal intensification of the easterly winds in the equatorial Atlantic. The year-to-year variability of this second seasonal cooling, called Atlantic Niño II by Okumura and Xie (2006), also results from a Bjerknes feedback. Anomalous westerly winds in the western equatorial Atlantic induce deepening of the thermocline in the eastern equatorial region and warming of surface waters (Okumura and Xie 2006). Contrary to the strong summer Atlantic equatorial mode, this second mode (called here winter Atlantic Niño) attracts much less attention. Although this winter mode is generally not the extension of the summer Atlantic Niño events (Okumura and Xie 2006), in some years both are of the same sign leading to a persistent-like Atlantic equatorial mode. It has been found that the winter Atlantic Niño is not significantly correlated with the contemporary Pacific ENSO. However, its several-month lead-lag teleconnection, at long-term period, with other tropical oceans has not been analyzed.

ENSO influences the tropical Atlantic and Indian basins via atmospheric bridge (Delécluse et al. 1994; Giannini et al. 2001; Alexander et al. 2002; Ashok et al. 2007; Yu and Lau 2005; Rodrigues et al. 2015; Tokinaga et al. 2019). For the Atlantic, the climatic impact is strong in the northern tropical part (Nobre and Shukla 1996; Enfield and Mayer 1997; Giannini et al. 2004; Park and Li 2019). ENSO also affects the variability of the South Atlantic Ocean, particularly the South Atlantic Dipole in winter when both ENSO and this dipole peak (Kayano et al. 2012; Rodrigues et al. 2015). According to Chang et al. (2006), there is a fragile relationship between the Pacific ENSO and the following equatorial Atlantic variability. Such weak teleconnection could result from a destructive interference between atmospheric and oceanic processes (Chang et al. 2006; Lübbecke and McPhaden 2012). Recently, Tokinaga et al. (2019) suggested that summer Atlantic Niño events can be triggered by multi-year ENSO events through atmospheric teleconnection. From these authors, during single-year ENSO events such teleconnection is not found between Pacific and Atlantic Niños. Nevertheless, other studies indicated some impact of ENSO over the Equatorial Atlantic, as for instance in Delécluse et al. (1994) for the Atlantic Niño of 1984, a potential subsequent event of the large 1982–1983 El Niño.

Several studies have also indicated the influence from other basins on the ENSO variability (Latif and Barnett 1995; Dong et al. 2006; Rodriguez-Fonseca et al. 2009; Izumo et al. 2010; Frauen and Dommenget 2012; Ham et al. 2013; Cai et al. 2019; Wang 2019). It has been shown that Atlantic Niño/Niña in summer have a leading influence, of opposite sign, on winter Pacific La Niña/El Niño events mainly from the 1970s climate shift (Rodriguez-Fonseca et al. 2009; Ding et al. 2012; Keenlyside et al. 2013; Polo et al. 2015a; Losada and Rodríguez-Fonseca 2016; Cai et al. 2019). Warm summer events in the equatorial Atlantic affect the Walker circulation with an ascending branch over the Atlantic and a descending branch over the central Pacific (Rodríguez-Fonseca et al. 2009; Ding et al. 2012; Polo et al. 2015a; Losada and Rodríguez-Fonseca 2016). The easterly wind anomalies induced by the descending branch of the Walker cell generate eastward propagating Kelvin waves and favor negative SST anomalies in the central and eastern Equatorial Pacific (Polo et al. 2015a). The opposite occurs during cold summer events in the equatorial Atlantic. Ding et al. (2012) have suggested that this Atlantic influence on ENSO also occurs before the 1970s. Other studies carried out over long study periods have indicated a non-stationarity of this relationship (Martín-Rey et al. 2014, 2015; Lübbecke et al. 2018). For instance, the lagged negative teleconnection between the Atlantic and Pacific Niños was strong during the first and last decades of the twentieth century, and weak between these periods. This non-stationarity of the Atlantic–Pacific teleconnection is suggested to be modulated by the AMO with strong negative relationships coinciding with negative AMO phases (Martín-Rey et al. 2014). However, it should be noted that the summer Atlantic Niño connection with ENSO persists through the positive AMO phase since 2000s (Jia et al. 2019).

Both Atlantic and Pacific Niños locally and remotely influence the South American climate variability through atmospheric perturbations (Uvo et al. 1998; Chiang et al. 2000; Kayano and Andreoli 2006; Grimm and Tedeschi 2009; Marengo et al. 2012; Rodrigues and McPhaden 2014; Kayano et al. 2011, 2012). Using summer ATL3 (3° N–3° S, 20° W–0°) SST anomalies, Hounsou-Gbo et al. (2019) have indicated its potential for predicting the following spring (February–April) rainfall in Northeast Brazil from 1980s onwards. According to these authors, the effect of summer ATL3 on the spring rainfall in Northeast Brazil is not direct and should depend on its teleconnection with the Pacific ENSO.

The main goal of the present study is to further investigate the leading influence of both summer and winter Atlantic

Niño over adjacent regional climates, including the Pacific ENSO. The long-term periods with strong and weak (or even inverse) relationships are identified. The mechanisms that relate the summer and winter Atlantic Niño (including persistent summer Atlantic Niño) to other tropical regions are explored.

Data and methods are presented in the following Section. In Sect. 3 we show the main results, with additional discussions about already known features, and new insights especially linked to the yearly lagged relationship between summer or winter Atlantic Niño and Pacific ENSO. We also analyze the impacts of the two types of Atlantic Niño events on South American climatic variability. A summary and conclusion are provided in Sect. 4.

2 Data and methodology

Observational and reanalysis ocean–atmosphere variables are used in this study. Observed SST (HadISST) and subsurface temperature (EN.4.2.1) datasets are from the Met Office Hadley Centre observations datasets. The 20 °C isotherm depth is considered as proxy for the thermocline depth. SST and subsurface temperature data extend over the period 1870 to present with the horizontal resolution of 1° × 1° (Rayner et al. 2003). These data are freely available at https://www.metoffice.gov.uk/hadobs/ at monthly timestep. Monthly pressure level winds and omega (vertical velocity) are from the Twentieth Century Reanalysis (20CR) spanning 1836–2015 with 1° latitude × 1° longitude horizontal grid and 24 pressure levels (Compo et al. 2011; Giese et al. 2016). We also used sea level pressure from 20CR. These data are available at https://www.esrl.noaa.gov/psd/data/gridded/data.20thC_ReanV3.html. Monthly precipitation from Global Precipitation Climatology Centre (GPCC) at 0.5° latitude × 0.5° longitude is available at https://www.esrl.noaa.gov/psd/data/gridded/data.gpcc.html and spans 1901 to the present (Schneider et al. 2013).

Monthly anomalies of all variables are obtained by removing the 30-year base climatology updated every 5 years. For example, anomalies during 1961–1965 are based on the 1946–1975 climatology, anomalies during 1966–1970 are calculated from the 1951–1980 climatology and anomalies from 2001 to the present are calculated using the 1986–2015 climatology. This kind of anomalies, also used for the calculation of the Oceanic Niño Index (ONI) by National Oceanic and Atmospheric Administration-Climate Prediction Center (NOAA-CPC; https://origin.cpc.ncep.noaa.gov/products/analysis_monitoring/ensostuff/ONI_change.shtml), has some advantages: The classification of past anomalies is not modified over the historical record, and all anomalies are based on their contemporary climatology. The long-term linear trend is also removed using updated climatology (Lutz et al. 2013).

In general, the definition of El Niño/La Niña in the Pacific is based on the genesis and duration of warm/cold SST anomalies in the central and eastern equatorial Pacific, mainly from fall to spring (Trenberth et al. 1997; Wolter and Timlin 1998; Cane 2005; L'Heureux et al. 2017; Santoso et al. 2017). On the other hand, it is known that the summer Atlantic Niño often does not persist for several months, until next winter (Zebiak 1993; Okumura et al. 2006; Lubbëcke et al. 2010; Polo et al. 2015b). Since the interannual variability of Atlantic Niño is relatively weak in term of magnitude and persistence compared to the Pacific El Niño, we define the Atlantic Niño (Niña) events as 3-month mean SST anomalies higher (lower) than + 0.35 °C (− 0.35 °C) in ATL3 region. Our definition of Atlantic Niño/Niña is slightly different from that of Lubbëcke et al. (2010) who considered monthly SST anomalies exceeding 70% of the standard deviation (0.5 °C) for at least three (3) months in summer. The threshold defined by Lübbecke et al. (2010) corresponds to ± 0.35 °C using NOAA Optimum Interpolation Sea Surface Temperature for the period 1982–2007.

For reasons related to our analysis, we split Atlantic Niño events that exceed the ± 0.35 °C threshold into non-persistent summer ATL3 (also called summer Atlantic Niño or JAS ATL3) and boreal fall/early winter ATL3 (also called winter Atlantic Niño or OND ATL3). The non-persistent summer Atlantic Niño are warm/cold events in JAS that do not persist until OND. We also tested the 3-month mean SST anomalies in JJA, which is the 3-month period of highest interannual variability (Lübbecke et al. 2010, 2018), to define the summer ATL3. There is no significant difference between the years selected using the JJA or JAS SST anomalies to define summer ATL3 events. Though, only the 3-month mean of JAS is considered here for summer Atlantic Niño because its correlation with the Pacific ENSO is slightly higher than that of JJA. The winter ATL3 are warm/cold events in OND, independently if they persist or not from JAS. Consequently, the winter ATL3 events used in this study also include persistent summer events (warm/cold persisting from JAS to OND). Also note that among the selected winter Atlantic Niño events, a few persist until the following spring. The results using persistent summer Atlantic Niño events are similar to those considering only winter ATL3 events, i.e., which do not persist from JAS (not shown). Therefore, in the following we analyze summer ATL3 and winter ATL3 events as two types of Atlantic equatorial modes.

Our study is mainly based on linear correlation and composite analyses using selected variables of ocean–atmosphere interaction to investigate the influence of summer and winter Atlantic Niño on ENSO and South American climate variability. The temporal evolution of the ATL3 (3° N–3° S, 20° W–0°) and Niño3 (5° N–5° S, 150° W–90°

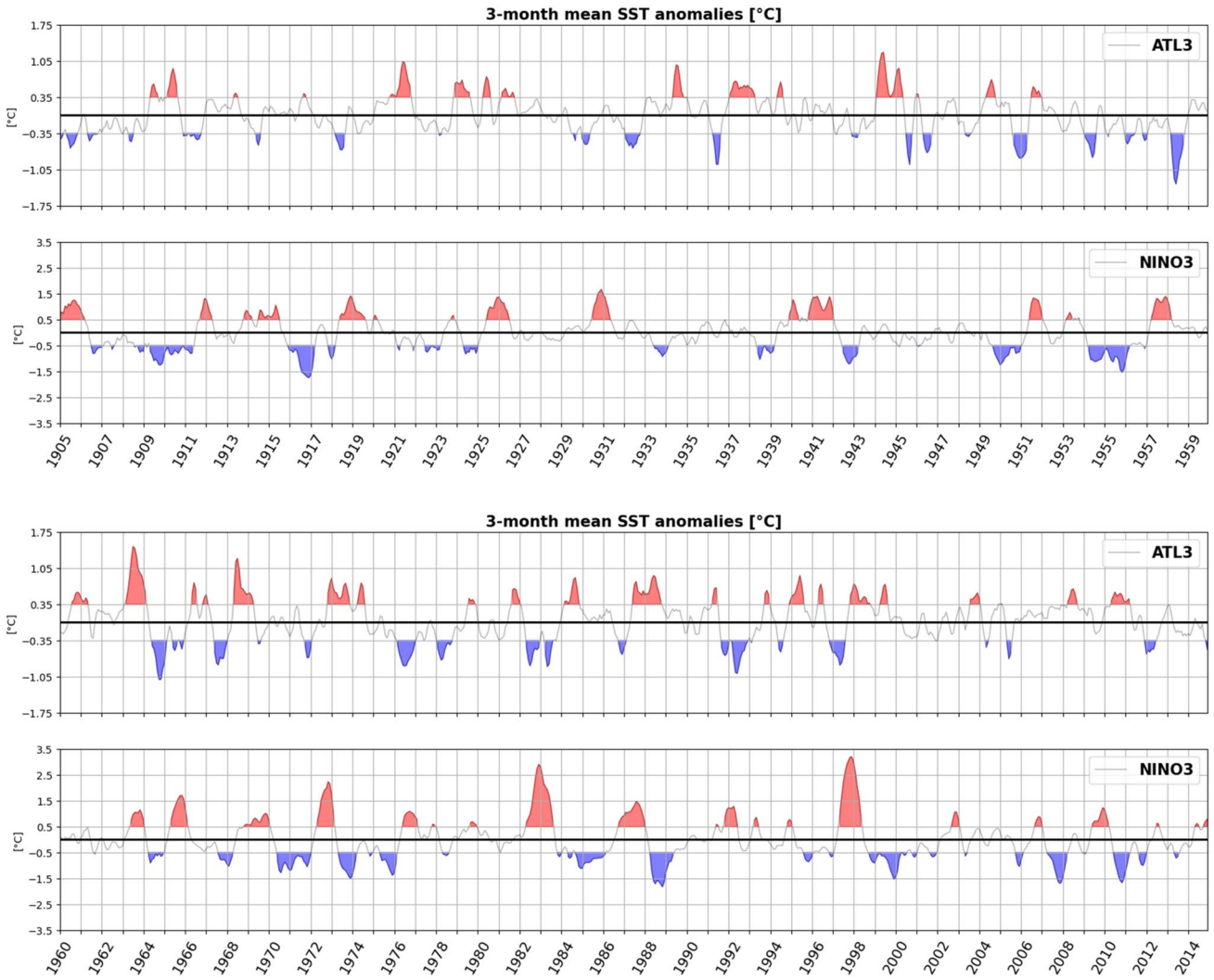

Fig. 1 Temporal evolution of the 3-month running mean of SST anomalies (in °C, from HadISST) for ATL3 (3° N–3°S, 20° W–0°) and Niño3 (5° N–5°S, 150° W–90° W) for the period 1905–2014. SST anomalies higher (lower) than + 0.35 °C (− 0.35 °C) in ATL3 region are filled in red (blue) and SST anomalies higher (lower) than + 0.5 °C (− 0.5 °C) in Niño3 region are filled in red (blue)

W) indices are indicated in the Fig. 1. All along this study, the seasons (three consecutive months) corresponding to the year of Atlantic Niño events are indicated by (0), e.g., July–August–September(0) [JAS(0)], and those of the year following the Atlantic Niño are indicated by (1), e.g., October–November–December(1) [OND(1)].

The 1905–2014 period, which overlaps HadISST, EN.4.2.1, 20CR and GPCC precipitation data, is used for the selection of ATL3 events considered for this study. These composites are based on the years of summer ATL3 and winter ATL3. All composites anomalies are the difference of composite of positive ATL3 events minus composite of negative ATL3 events. Therefore, the sign of all composites corresponds to positive ATL3 conditions. According to this selection criterion, 10 positive (i.e. warm events) and 14 negative (cold events) JAS ATL3 events were considered (see Table 1). In the same manner, 15 positive and 10 negative OND ATL3 events were selected. It should be noted that we exclude the years of consecutive winter and summer events having the same sign, i.e., OND(0) ATL3 followed by JAS(1) ATL3 of the same sign. These years are; for positive events: OND1920–JAS1921, OND1973–JAS1974, OND1987–JAS1988, OND1997–JAS1998; for negative events: OND1905–JAS1906, OND1982–JAS1983, OND1996–JAS1997. Analyzing the Table 1 in detail, it can be seen that the 10 positive JAS ATL3 are relatively well distributed during the first half of the twentieth century, subsequently rare until the 1990s, and more again until the present time (see also Fig. 1). The 14 negative JAS ATL3 are evenly distributed over the study period. The 15 positive OND ATL3 are relatively well distributed throughout the study period, except during the first three decades of the

Table 1 Years of non-persistent summer ATL3 (JAS ATL3) and winter ATL3 (OND ATL3), according to the adopted ± 0.35 °C criteria

ATL3 events	Years
Positive JAS (**10**)	1909, 1910, 1924, 1925, 1926, 1939, 1949, 1995, 1999, 2008
Positive OND (**15**)	**1934**, **1937**, **1944**, **1951**, **1960**, **1963**, 1966, **1968**, 1972, **1979**, 1981, **1984**, 1993, **2003**, **2010**
Negative JAS (**14**)	1911, 1914, 1918, 1929, 1932, 1936, 1945, 1946, 1948, 1954, 1958, 1969, 1978, 1994
Negative OND (**10**)	1950, 1956, **1964**, 1965, **1967**, 1971, **1976**, 1986, 1991, **1992**

Bold corresponds to OND ATL3 that persisted from JAS

twentieth century. The negative OND ATL3 are very few until the middle of the twentieth century and in the beginning of the twenty-first century, fairly regularly represented between these two periods. It should also be noted that OND events (positive or negative) are best represented in decades of the middle of the twentieth century. Many of the positive OND ATL3 events persisted from JAS, most of them having been observed in decades of the mid-twentieth century, whereas the negative OND ATL3 are generally independent of the summer events.

3 Results

3.1 Multidecadal changes in the influence of summer and winter Atlantic Niño on ENSO

First, we analyze the relationship between the winter ATL3 and Niño3. Figure 2a displays the lead-lag correlation, with 25-year sliding window, between OND(0) ATL3 and Niño3 for the 1905–2014 period. It appears that the winter ATL3 is significantly negatively correlated (black dotted line) with the following Niño3 during several decades. Nonetheless, a multidecadal modulation of the lead time of the significant negative relationship is clearly noticeable. The longest lead time, i.e. nearly 1-year lead, is marked from 1940 to 1970s while the shortest lead time of about 6-month is observed before and after this period. These results indicate the existence of a leading connection between the winter ATL3 and the following year ENSO. However, the multidecadal change of the lead time suggests that the winter ATL3 can modulate the development of ENSO from early summer to winter. Although positive correlation is noted during the 1930–1970s, no significant values are noted when Niño3 leads the winter ATL3. This observation shows that the relatively weak influence of ENSO on the variability of winter ATL3 also exhibits a multidecadal modulation. We also analyze the connection between ATL3 in other seasons (i.e., JFM, AMJ, JAS) and ENSO (not shown). For these seasons, negative significant negative correlations are found, when the Atlantic leads the Pacific by several months, only during the first and last decades of the study period.

In order to highlight the differences between these results and previous studies we examine the multidecadal modulations of the lagged relationship between the summer and winter Atlantic Niño and the Pacific ENSO at different lag times. The first relationship is the lagged correlation between JAS(0) ATL3 and the subsequent OND(0) Niño3 (orange line in Fig. 2b). The negative relationship between these events is significant ($r < -0.45$) during the first and last decades of the twentieth century, in agreement with previous results (e.g. Martin-Rey et al. 2014, 2015; Lübbecke et al. 2018). Such negative correlation remains significant during the beginning of the present century. Inversely this lagged relationship is weakly negative ($r > -0.2$), or even weakly positive ($r < +0.2$) during decades of the middle of the twentieth century (basically from 1930 to 1970s). Martín-Rey et al. (2014) have suggested that this multidecadal variation of the negative correlation between the summer Atlantic Niño and ENSO is modulated by the AMO.

The second relationship is the multidecadal evolution of the 1-year lead correlation between OND(0) ATL3 and OND(1) Niño3 (black line in Fig. 2b). Interestingly, a multidecadal modulation of this 1-year lead correlation is also marked. The significant negative values ($r < -0.45$) are generally observed between 1940 and 1970s (see also Table 1), thus the core of the decades corresponding to the lower relationship between summer ATL3 and the subsequent OND(0) Niño3 (black line vs. orange line). These results suggest that the connection between Atlantic equatorial modes and ENSO exists all along the 110-year study period. However, the relationships of the summer and winter ATL3 with ENSO are complementary at multidecadal timescale: generally, when one is highly negative the other is low, and conversely.

Because our study is mainly based on two types of Atlantic Niño, i.e. summer and winter events, we analyze the multidecadal variation of the correlation between them. The green line in Fig. 2b is the 25-year sliding window correlation between JAS ATL3 and OND ATL3. The persistence of Atlantic Niño presents a slow multidecadal variation along the 110-year study period. During the first decades of the twentieth century, as well as during the last decades of this century and the first years of the present century, the

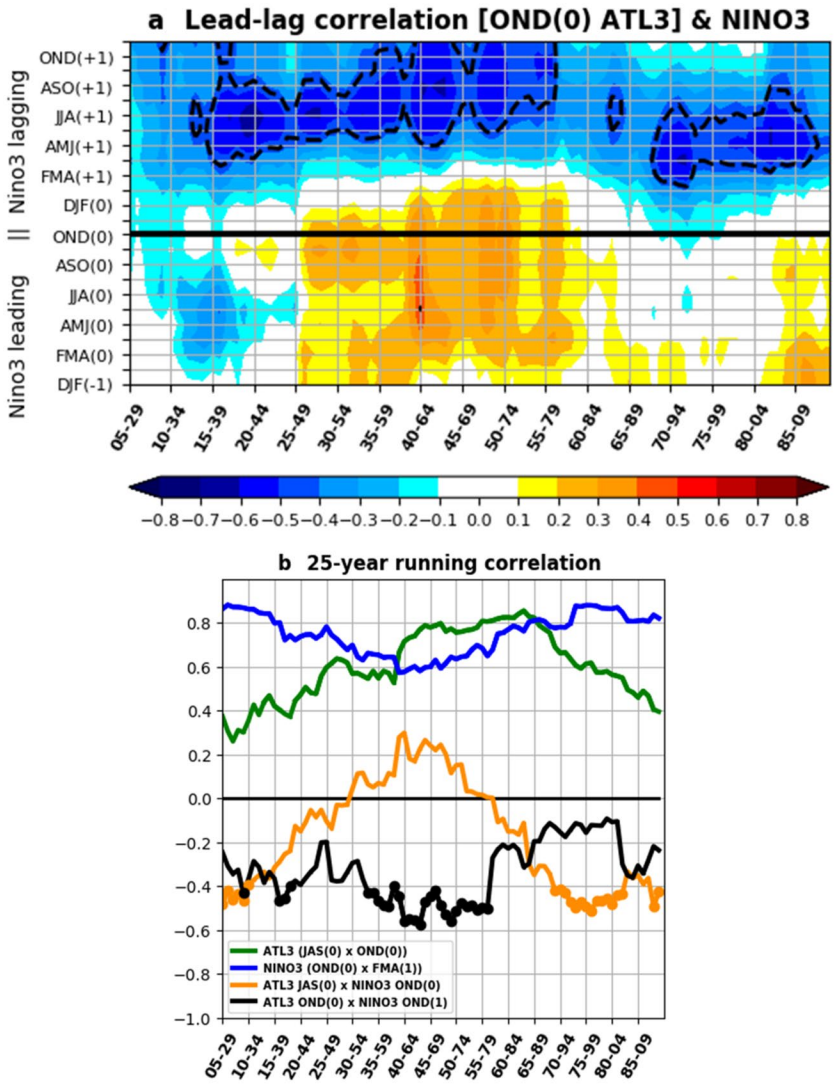

Fig. 2 **a** Lead–lag correlation, with a 25-year sliding window, between October–December [OND(0)] ATL3 (3° N–3° S, 20° W–0°) and Niño3 (5° N–5° S, 150°–90° W) SST indices. The values in the y-axis are the 3-month mean of Niño3. The horizontal black line at OND(0) indicates the zero-lag correlation between OND(0) ATL3 and OND(0) Niño3. Values below OND(0) indicate Niño3 leading the OND(0) ATL3. Values above OND(0) indicate Niño3 lagging OND(0) ATL3. Contours show correlation significant at 95% confidence level using t-test; **b** Evolutions of the 25-year sliding window correlation between JAS(0) ATL3 and OND(0) ATL3 (green line), OND(0) Niño3 and FMA(1) Niño3 (blue line), JAS(0) ATL3 and OND(0) Niño3 (orange line), and the OND(0) ATL3 and OND(1) Niño3 (black line). Each value in x-axis (**a** and **b**) represents the running correlation of 25 consecutive years. For instance, the first value at 05–29 represents the correlation of events from 1905 to 1929, the second values at 06–30 corresponds to the correlation of events of 1906–1930, and so on. Dots in the orange and black lines in **b** indicate correlation significant at 95% confidence level using t-test. SST are from HadISST for the period 1905–2014

persistence of ATL3 from summer to fall/early winter is relatively weak with values lower than + 0.5. The correlation is strong (r > + 0.6) from the 1930s to the 1980s. These results suggest that summer and winter Atlantic Niño are generally not separated events particularly during these decades. However, they appear to be more independent during the first and last decades of the study period. This observation justifies why ATL3 events are split into non-persistent summer and winter events in the present study. The winter ATL3 events are not only events limited to the winter but they also include persistent summer events (i.e. warm/cold ATL3 persisting from summer to winter). One of the reasons for including persistent summer events in the winter events is that during the decades of long persistence of summer ATL3 events, only winter ATL3 anomalies are significantly correlated with ENSO in year(1). These results support a multidecadal

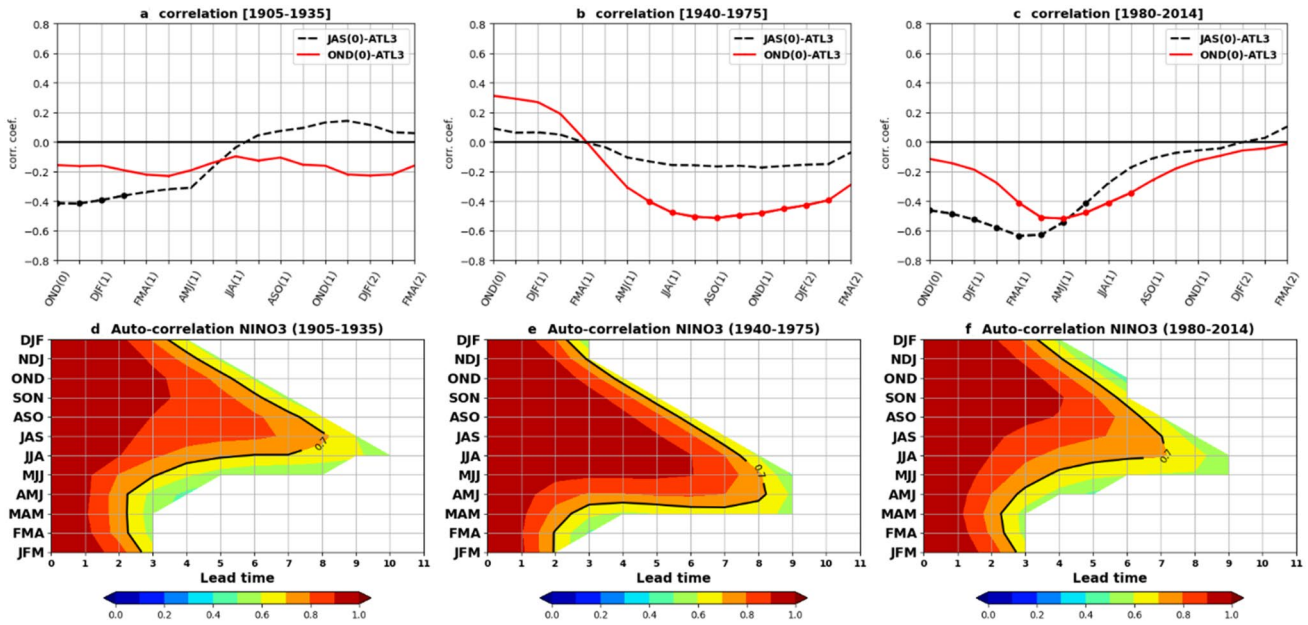

Fig. 3 **a**–**c** Evolution of the linear correlation coefficient between: JAS(0) ATL3 and 3-month Niño3 from OND(0) to FMA(2) (black dashed line); OND(0) ATL3 and Niño3 from OND(0) to FMA(2) (red line) for: **a** 1905–1935, **b** 1940–1975 and **c** 1980–2014 periods. Note that the correlation starts at 3-month lead (JAS(0), ASO(0) and SON(0) correlations are not shown) for the JAS ATL3 and at 0-month lead for the OND ATL3. SST is from HadISST for the 1905–2014 period. Dots indicate correlation significant at 95% confidence level using t-test. **d**–**f** Auto-correlation of Niño3 as function of lead time (x-axis) and 3-month anomalies (y-axis) for: **d** 1905–1935, **e** 1940–1975 and **f** 1980–2014 periods. The black contour in **d**–**f** indicates correlation of + 0.7. Only correlation significant at 99% confidence level is shown for **d**–**f**

modulation of the equatorial Atlantic variability. The longer duration of the Atlantic Niño from summer to winter may be due to its later development during the decades of the mid-twentieth century (not shown). According to Martín-Rey et al. (2018), the Atlantic Niño variability is modulated by the AMO. For negative phases of the AMO, summer SST anomalies in the equatorial Atlantic are enhanced and extend westward, while the Atlantic Niño is restricted to the eastern equatorial Atlantic for positive phases of the AMO (Martín-Rey et al. 2014). It is suggested that these changes in equatorial Atlantic variability are associated with changes in atmospheric circulation related to tropical teleconnections (Losada and Rodríguez-Fonseca 2016).

As in the case of ATL3, we also analyze the multidecadal variation of the persistence of Niño3 from fall/early winter (OND) to spring (February–April, FMA) (Fig. 2b, blue line). The correlation between OND Niño3 and FMA Niño3 is very strong ($r > +0.7$) during the first and last decades of the 1905–2014 study period. Thus, when the summer ATL3 are significantly correlated with the subsequent winter ENSO (Fig. 2b, blue line vs. orange line). The persistence of Niño3 is generally relatively lower ($r < +0.7$) from 1930 to 1960s, when the lagged relationship between summer ATL3 and the subsequent OND(0) Niño3 is weak. Interestingly, the 1-year lead correlation between OND(0) ATL3 and OND(1) Niño3 is higher ($r < -0.5$; black line in Fig. 2b) when summer ATL3 is not significantly correlated with the subsequent OND(0) Niño3 (Fig. 2b, black line vs. orange line). The same analysis of the multidecadal evolution of the persistence of Niño3 but from MJJ to OND shows an opposite behavior: high persistence is observed in the decades of the middle of the twentieth century while relatively least persistence is observed in the first and last decades of the study period (not shown). This suggests that the winter Niño3 is more related to the previous summer Niño3 in decades of the mid-twentieth century than before and after these decades.

In order to highlight the influence of the two types of Atlantic Niño on the Pacific ENSO during certain decades we divide the 1905–2014 study period into 3 sub-periods (1905–1935, 1940–1975 and 1980–2014) based on the significant correlations. Since ENSO is known to present a seasonal dependence of its persistence (An and Wang 2001; McPhaden 2003; Ren et al. 2016), we also analyze the seasonality of the persistence of Niño3 for each of the 3 sub-periods considered.

For the 1905–1935 period, the JAS(0) ATL3 is significantly negatively correlated with the fall to late winter Niño3 (black dots in black line in Fig. 3a). This correlation remains weakly negative from spring [FMA(1)] to summer [JJA(1)] and becomes positive ($r < +0.2$, not significant) from summer(1) until the end of the year(1). The Niño3

Table 2 Hindcast of Niño3 SST anomalies based on cross-validated (leave one out cross-validation) simple linear regression model using: JAS(0) ATL3 SST anomalies as predictor (top panel); and OND(0) ATL3 SST anomalies as predictor (bottom panel)

Hindcast of Niño3 using JAS(0) ATL3 SST anomalies as predictor													
Niño3 seasons		ASO0 Lead + 1	SON0 Lead + 2	OND0 Lead + 3	NDJ0 Lead + 4	DJF1 Lead + 5	JFM1 Lead + 6	FMA1 Lead + 7	MAM1 Lead + 8	AMJ1 Lead + 9	MJJ1 Lead + 10	JJA1 Lead + 11	JAS1 Lead + 12
1905–1935	Corr	0.28	0.30	0.27	0.28	0.25	0.21						
	rmse/std	0.97	0.97	0.98	0.97	0.97	0.99						
1940–1975	Corr												
	rmse/std												
1980–2014	Corr		0.26	0.31	0.34*	0.41*	0.48*	0.56*	0.55*	0.44*	0.26		
	rmse/std		0.98	0.96	0.95	0.92	0.89	0.83	0.84	0.90	0.97		
Hindcast of Niño3 using OND(0) ATL3 SST anomalies as predictor													
Niño3 seasons		JFM1 Lead + 3	FMA1 Lead + 4	MAM1 Lead + 5	AMJ1 Lead + 6	MJJ1 Lead + 7	JJA1 Lead + 8	JAS1 Lead + 9	ASO1 Lead + 10	SON1 Lead + 11	OND1 Lead + 12	NDJ1 Lead + 13	DJF2 Lead + 14
1905–1935	Corr												
	rmse/std												
1940–1975	Corr					0.32	0.41*	0.44*	0.45*	0.43*	0.42*	0.38*	0.36*
	rmse/std					0.95	0.91	0.90	0.89	0.90	0.91	0.93	0.94
1980–2014	Corr			0.37*	0.40*	0.35*	0.24						
	rmse/std			0.94	0.93	0.95	0.99						

Indicated are the correlation coefficients (corr.) between predicted and observed Niño3 SST anomalies; and rmse/std (ratio of the root-mean-square-error to the standard deviation of observed Niño3) for different 3-month mean for the 1905–1935, 1940–1975 and 1980–2014 periods. Correlations are shown only where the corresponding rmse/std is lower than 1. Correlations significant at 95% confidence level using t-test are indicated by *. Note the difference in the target 3-month for JAS and OND ATL3 cases

SST anomalies predicted by a cross-validated linear regression model using JAS(0) ATL3 as predictor also presents a similar behavior (Table 2). However, the correlation coefficients between the predicted Niño3 and observed Niño3 (r ~ 0.2–0.3) from ASO(0) to JFM(1) are not significant. The OND(0) ATL3 is weakly negatively correlated with Niño3 (r ~ − 0.2) from OND(0) to FMA(2) (red line Fig. 3a). Therefore, OND(0) ATL3 has no ability to predict Niño3 for the 1905–1935 period (Table 2). The persistence of the Niño3 is weak (lead time ~ 2 months) for SST anomalies starting from JFM to MJJ, basically in spring/early summer, considering correlation coefficients > + 0.7 (Fig. 3d). This persistence becomes strong with lead time of about 8 months for SST anomalies starting in summer, more specifically in JAS, indicating that summer SST anomalies can be highly correlated with those of the following winter. From JAS onwards, the persistence of Niño3 decreases almost linearly from 8 months for SST anomalies starting in JAS to 3 months for SST anomalies starting in JFM. The short persistence of SST anomalies starting in spring is known as spring persistence barrier (McPhaden 2003; Jin et al. 2008; Ren et al. 2016).

During the 1940–1975 period, there is no significant correlation between the JAS(0) ATL3 and Niño3 from OND(0) up to FMA(2) (Fig. 3b, black dashed line). This observation corroborates the non-significant correlation between the JAS(0) ATL3 and the subsequent Niño3 observed during the decades of the middle of the twentieth century (orange line in Fig. 2b). Thus, summer Atlantic Niño has no ability to forecast Niño3 during these decades (Table 2) as also indicated by previous results (Martín-Rey et al. 2014, 2015; Lübbecke et al. 2018). For OND(0) ATL3, weak positive correlation is observed with Niño3 from OND(0) to FMA(1) (red line in Fig. 3b). Although not significant, the positive correlation observed when winter ATL3 and Niño3 are in phase (0-month lead) suggests a positive relationship between them in this period. To a certain extent, Niño3 also influences positively the winter ATL3 as indicated in Fig. 2a even if this impact appears to be relatively weak. The correlation of winter ATL3 with the following Niño3 becomes negative from MAM(1) to FMA(2) with significant values (r < − 0.4) observed from MJJ(1) to JFM(2) (red dots in red line in Fig. 3b). Interestingly, the strongest negative correlation of winter OND(0) ATL3 with Niño3 (r ~ − 0.5) is found in the following fall [ASO(1)], i.e. with 10-month lead. This suggests that the winter ATL3 is connected with Niño3 from summer to winter in the mid-twentieth century. Our results suggest that ENSO events that develop early tend to terminate rapidly after the mature phase, although this observation is not symmetrical for warm and cold equatorial Pacific events (Okumura and Deser 2010; Wu et al. 2019). The Niño3 SST anomalies predicted using the OND ATL3 as predictor leads to the same conclusion, with the highest correlation between predicted and observed Niño3 (r ~ 0.45) in ASO(1) (Table 2). The persistence of Niño3 also exhibits a noticeable seasonality during these decades. However, the least persistence is marked in late winter/early spring (from DJF to MAM) (Fig. 3e). This indicates that the persistence barrier in SST occurs earlier in the calendar year during the decades of the mid-twentieth century compared to the 1905–1935 period. The longest duration, for the 1940–1975 period, is marked for SST anomalies starting in AMJ-MJJ with a lead time of about 8 months. Clearly, the 3-month SST anomalies of the longest persistence are also observed earlier in the calendar year. This observation indicates that SST anomalies that start in AMJ-MJJ can persist until the following winter and also supports an early development of ENSO during these decades. Therefore, we argue that the fact that SST anomalies starting in late spring/summer can persist into the following winter contributes to the nearly 1-year lead correlation between OND(0) ATL3 and OND(1) Niño3.

During the recent decades (1980–2014), significant negative correlation is observed between the JAS(0) ATL3 and Niño3 from OND(0) to MJJ(1) with the strongest value (r ~ − 0.6) in spring (FMA(1), ~ 7-month lead) (black line in Fig. 3c). This correlation remains negative but not significant from JJA(1) to winter(1) and becomes weakly positive in the beginning of the year(2). The highest correlation (r ~ 0.55) between the Niño3 predicted using JAS(0) ATL3 as predictor and observed Niño3 is noted in FMA(1)–MAM(1), i.e. about 7-month lead (Table 2). This prediction of the Niño3 SST anomalies using summer Atlantic Niño as predictor is similar to that of previous studies although the periods considered are slightly different (Martín-Rey et al. 2014, 2015). The OND(0) ATL3 is negatively correlated with Niño3 from OND(0) to the end of year(1) (red line in Fig. 3c). The negative correlation is significant from FMA(1) to JAS(1) with strongest value (r ~ − 0.5) in AMJ(1) (Fig. 3c, red dots in red line). The correlation between the Niño3 predicted using OND(0) ATL3 as predictor and the observed Niño3 is significant from MAM(1) to MJJ(1) with highest value (r ~ 0.4) in AMJ(1) (Table 2). Therefore, both JAS(0) and OND(0) ATL3 appear to be significantly connected with Niño3 during the recent decades although the influence of the summer ATL3 is clearly stronger than that of winter ATL3. The JAS ATL3 appears to be highly connected with Niño3 from winter to spring while the OND ATL3 is mainly related to Niño3 from late spring to summer for the 1980–2014 period. This observation is also valid when the entire 1905–2014 study period is considered (not shown). Yet, the highest correlation of winter ATL3 with Niño3 in summer JJA(1) (r ~ − 0.4) is stronger than that of the summer ATL3 with Niño3 in spring FMA(1) (r ~ − 0.25) for the 1905–2014 period. The persistence of

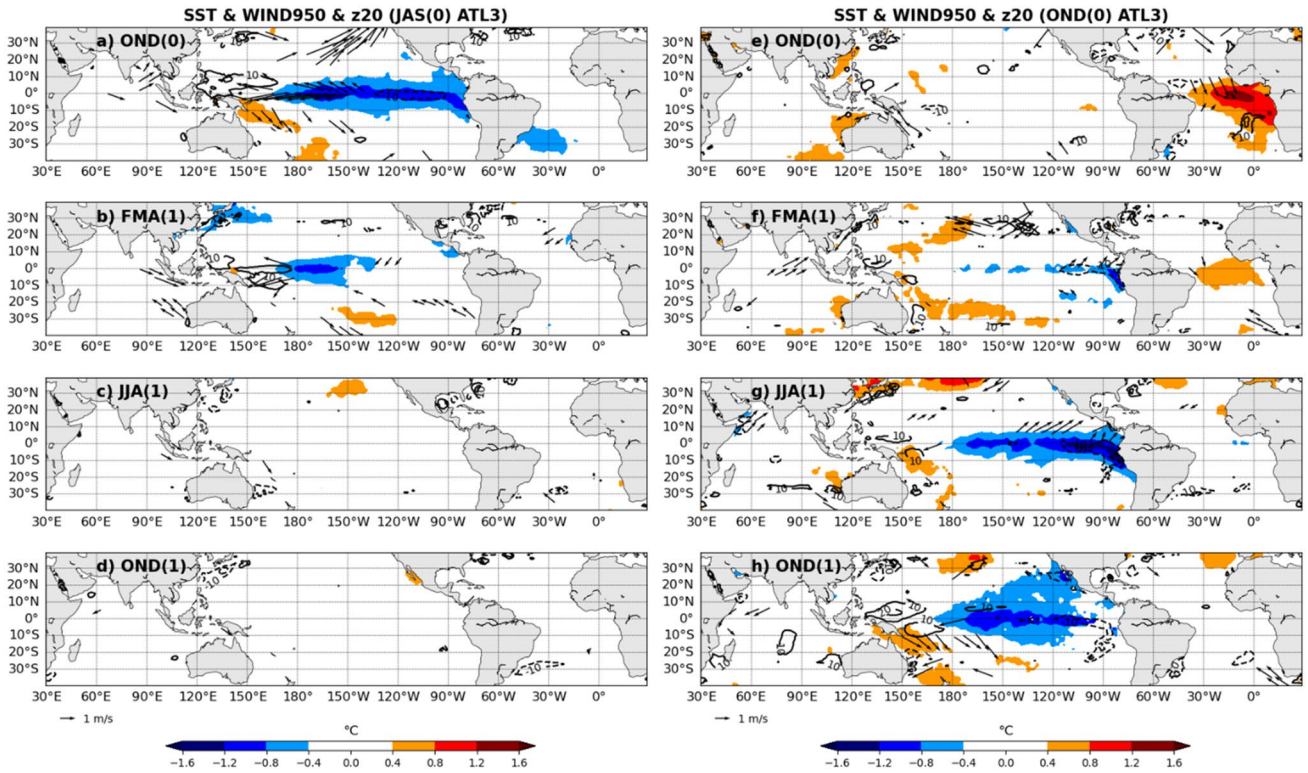

Fig. 4 Difference of composite SST (shading, °C), surface wind (950 hPa, vectors, m/s) and 20 °C isotherm depth (z20, contours, m) anomalies in OND(0), FMA(1), JJA(1) and OND(1) for: (left panels; **a**–**d**) JAS(0) ATL3; and (right panels; **e**–**h**) OND(0) ATL3. The difference is based on composite of positive ATL3 minus composite of negative ATL3. SST, wind and z20 are respectively from HadISST, Twentieth-Century Reanalysis product (20CR) and EN.4.2.1 (subsurface temperature) for the 1905–2014 period. Dashed/full lines indicate negative/positive values for z20 anomalies higher than ± 10 m. Only difference significant at 95% and 90% confidence level according to Welch's test is shown for SST and wind anomalies respectively

Niño3, for the period 1980–2014, is similar to that of the 1905–1935 period with a shorter persistence (< 3 months) for SST anomalies starting in JFM–AMJ and a longer persistence of about 7 months for anomalies starting in JJA–JAS (Fig. 2f). Moreover, contrary to the 1940–1975 period, the influence of OND(0) ATL3 on Niño3 for the 1980–2014 period is limited to spring/early summer, i.e. during the spring persistent barrier (dots in red line Fig. 3c vs. Fig. 3f). The short duration of the influence of the OND ATL3 on ENSO seems to be associated with a persistence barrier extending to early summer during the recent decades. Competition between the influences of summer and winter Atlantic Niño on ENSO, among others mechanisms, could also explain these observations. Nevertheless, these observations deserve more detailed studies.

In general, the teleconnection between the Atlantic and Pacific Niños is associated with the variability in each basin. It coincides with low (high) persistence of the summer Atlantic Niño index (green line in Fig. 2b) and high (low) persistence of the winter Pacific Niño index (green line in Fig. 2b). Thus, a significant negative connection between summer Atlantic Niño and the subsequent winter Pacific ENSO is associated with shorter duration of summer ATL3 and longer duration of winter Niño3. The inverse occurs when the winter Atlantic Niño is significantly correlated with the nearly 1-year lag Pacific ENSO. The Niño3 persistence barrier also seems to show a shift during certain decades. In the decades of the mid-twentieth century the persistence barrier is observed early in the calendar year while it appears relatively late during the first and last decades of the study period. These observations support a complex inter-basin connection between the equatorial Atlantic and Pacific at multidecadal timescale (Polo et al. 2015a; Losada and Rodríguez-Fonseca 2016; Cai et al. 2019; Wu et al. 2019).

3.2 On the mechanism of Atlantic–Pacific teleconnections

In order to examine the mechanisms of teleconnection between the two types of Atlantic Niño and the global tropical oceans, we analyze the composites of selected ocean–atmosphere variables in the tropics for the 1905–2014 period. We did not limit the composites analysis to specific

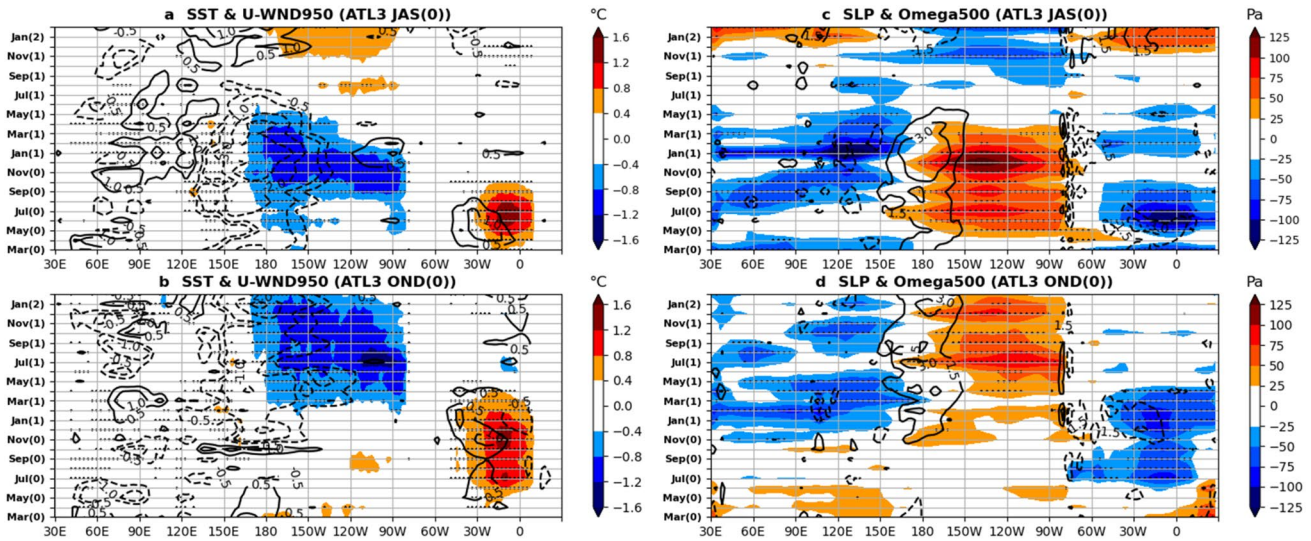

Fig. 5 Longitude-time diagram of the difference of composite of: (left panels; **a** and **b**) SST (shading, °C) and zonal wind (contours, m/s) anomalies; (right panels; **c** and **d**) sea level pressure (shading, Pa) and 500 hPa vertical velocity (negative upward, contours, 10^{-2} Pa/s) anomalies. Top panels (**a** and **c**) are for JAS(0) ATL3 and bottom panels (**b** and **d**) are for OND(0) ATL3. All anomalies are averaged between 3° N–3° S. Dashed/full lines indicate negative/positive values for zonal wind and vertical velocity anomalies. Black dots indicate difference significant at 90% confidence level according to Welch's test for SST and SLP anomalies

decades since the influence of both summer and winter Atlantic Niño on ENSO can also be observed outside the sub-periods selected above (Table 1). Figure 4 displays the differences (positive ATL3 minus negative ATL3) of composite SST, surface wind (950 hPa) and 20 °C isotherm depth (z20) anomalies in all the tropics corresponding to JAS and OND Atlantic Niño. The maps in Fig. 4 are shown for OND(0), FMA(1), JJA(1) and OND(1), i.e. skipping one month, in order to reduce the number of maps. For the composites based on JAS(0) ATL3, significant positive anomalies of SST are observed only in JAS(0) in the equatorial Atlantic (not shown). For the composites based on OND(0) ATL3, significant positive signal is also observed in the equatorial Atlantic in JAS(0) because the OND ATL3 events selected here also include persistent JAS ATL3 events.

For the composite based on JAS(0) ATL3, the corresponding composite of wind anomalies indicates significant anomalous easterly wind in the central equatorial Pacific (150°–180° W) during the following OND(0) (Fig. 4a). The anomalous easterly wind is associated with shallower thermocline in the eastern equatorial Pacific and deeper thermocline in the west. This shoaling of the thermocline in eastern equatorial Pacific is generated by eastward propagating Kelvin waves (Polo et al. 2015a; Wu et al. 2019). The anomalously shallow thermocline in the east is associated with negative SST anomalies in the central and eastern equatorial Pacific. Significant positive SST and westerly wind anomalies are also observed in the southwestern tropical Pacific. In the following spring [FMA(1)], relatively weak negative SST anomalies are observed in the central equatorial Pacific, indicating the decay phase of the ENSO (Fig. 4b). No SST anomalies are present in the Pacific during the next year summer [JJA(1)) and winter (OND(1)] (Fig. 4c, d). Visibly, the case of JAS(0) ATL3 corresponds to the lagged negative relationship between the summer Atlantic Niño and the following winter Pacific ENSO largely documented (Rodríguez-Fonseca et al. 2009; Ding et al. 2012; Martín-Rey et al. 2014, 2015; Polo et al. 2015a; Losada and Rodríguez-Fonseca 2016; Lübbecke et al. 2018; Cai et al. 2019).

For the composite based on OND(0) ATL3, a positive SST signal is clearly present in the equatorial and southeastern tropical Atlantic (Fig. 4e). This warm SST signal is associated with westerly wind anomalies north and south of the western equatorial Atlantic region. No significant SST and surface wind anomalies are present in the Pacific in OND(0), except in the southeast equatorial region where southeasterly wind are noted (Fig. 4e). In FMA(1), positive SST anomalies (< 0.8 °C) remains in the south equatorial Atlantic and weak negative SST anomalies are observed east of 120° W in the equatorial Pacific (Fig. 4f). In the next summer [JJA(1)] and winter [OND(1)], significant negative SST anomalies occur in the equatorial Pacific (Fig. 4g, h). These negative SST anomalies are related to anomalous easterly wind in the central Pacific around 180° W. In this case, an increased thermocline slope is also observed with positive anomalies in the western and negative anomalies in the eastern equatorial Pacific. It is important to note that, for the OND(0) ATL3, the strongest SST anomalies are observed in summer/fall in the eastern equatorial Pacific as also indicated in Fig. 3b, e. Consequently, the OND(1)

SST anomalies (Fig. 4h) observed in the equatorial Pacific correspond to the decay phase of ENSO, which develops earlier in the calendar year. Clearly, as in the classical summer Atlantic vs. ENSO, the Bjerknes feedback also operates in the equatorial Pacific during OND(1) ATL3 events. In contrast to the JAS(0) events, the OND(0) Atlantic equatorial events are significantly connected to the following year Pacific ENSO (left panels vs. right panels Fig. 4).

Figure 5 displays longitude-time diagrams of the difference of composites anomalies of different variables averaged between 3° N and 3° S along the full equatorial region from March(0) until February(2). The variables used are SST, zonal wind at 950 hPa, SLP and vertical velocity at 500 hPa (negative upward). These variables are analyzed for both summer Atlantic Niño (Fig. 5, top panels) and winter Atlantic Niño (Fig. 5, bottom panels).

For the composite based on JAS(0) Atlantic Niño (Fig. 5a), we observe significant positive signal of SST from March(0) to September(0) in the equatorial Atlantic region. These positive SST anomalies are associated with anomalous westerly surface zonal wind in the western equatorial Atlantic. This corroborates results by previous studies that indicated that the Atlantic equatorial mode of SST is triggered by zonal wind anomalies in the west Atlantic (Servain et al. 1982, 1998, 1999; Zebiak 1993). In the equatorial Pacific, negative SST anomalies are observed in the central part from April(0) for a year until April(1). During that period, around November–December(0), strong negative SST anomalies (i.e. La Niña signal) are observed in the eastern equatorial Pacific. These negative anomalies are related to a long period of anomalous easterly wind in the central Pacific from spring(0) to fall(1). The largest easterly wind anomalies (> 2 m/s) are located between 150° E and 150° W in late fall(0) and early winter(0).

The evolution of the difference of composites of SLP anomalies is in agreement with that of the SST anomalies for JAS(0) Atlantic Niño events (Fig. 5c). Thus, negative (positive) SLP anomalies are broadly located in regions of positive (negative) SST anomalies in the equatorial Atlantic and Pacific oceans. Other negative anomalies of the SLP are observed in the equatorial Atlantic in January(1) and in the western equatorial Pacific and Indian Ocean from fall(0) to spring(1). The composites of 500 hPa vertical velocity anomalies indicate upward (negative) motion in the Atlantic during spring(0) (Fig. 5c). Large descending motion (positive vertical velocity; $> 1.5\ 10^{-2}$ Pa/s) is found in the central Pacific (150° E–150° W) from spring(0) to spring(1), with maximum in fall-winter(0). The high negative values of the vertical velocity around 80° W in Fig. 5c is mainly due to the Andes Cordillera. Once more, the well-known Atlantic–Pacific lagged negative teleconnection, which acts through perturbation in the Walker circulation, is evidenced for JAS(0) ATL3 with the Bjerknes feedback identifiable in both equatorial Atlantic and Pacific (Fig. 5a, c).

For the composite based on winter Atlantic Niño, positive composites of SST anomalies are present in the eastern equatorial Atlantic from late spring(0) to early spring(1) with the strongest values (> 1.2 °C) limited to winter(0) (Fig. 5b). The positive SST anomalies are associated with several months of anomalous westerly surface winds in the western part of the basin. A first peak of anomalous westerly wind is strong (> 0.5 m/s) in late spring and early summer and the second one (> 0.5 m/s) is observed from winter(0) to spring(1) with strongest value (> 1 m/s) in November(0). The second anomalous westerly wind should correspond to the trigger of the winter Atlantic Niño identified by Okumura and Xie (2006). In the equatorial Pacific, no significant value of composites of SST anomalies is noted during the months corresponding to the positive values in the equatorial Atlantic. Nonetheless, large significant negative values extend from spring(1) to the end of the year(1). No significant surface zonal wind anomalies are identified in the equatorial Pacific during the summer and fall of the year(0) (Fig. 5b). Anomalous easterly wind are observed from November(0) to winter(1) in the central and western equatorial Pacific.

The longitude-time evolution of SLP anomalies corresponding to the OND(0) ATL3 (Fig. 5d) are similar (with opposite sign) to that of SST anomalies in Fig. 5b. Negative SLP anomalies are observed in the Atlantic from summer(0) to spring(1) and positive anomalies are noted in the equatorial Pacific from spring(1) to winter(1). Negative anomalies are also observed in the western equatorial Pacific and in the equatorial Indian Ocean in winter(1). The evolution of the 500 hPa vertical velocity shows ascending motion ($< -1.5\ 10^{-2}$ Pa/s) in the western equatorial Atlantic in winter(0) and spring(1) (Fig. 5d). In the equatorial Pacific, strong descending motion ($> 1.5\ 10^{-2}$ Pa/s) extends a year-long from winter(0) to winter(1) around the dateline. We argue that a same mechanism of the Atlantic–Pacific Niño teleconnection operates during both JAS(0) ATL3 and OND(0) ATL3 events. Positive/negative SST anomalies in the ATL3 region induce simultaneously anomalous ascending/descending motion in the equatorial Atlantic and lagged anomalous descending/ascending motion in the central equatorial Pacific. However, in the case of winter Atlantic Niño, the significant oceanic response of equatorial Pacific to perturbation in the Walker circulation starts in late spring. Therefore, as indicated above, the winter Atlantic Niño is associated with early development of ENSO. The nearly 3-month delay between the OND(0) ATL3 and the oceanic response of equatorial Pacific may be due to the weak interaction between ocean and atmosphere in spring (Zebiak and Cane 1987; Blumenthal 1991) the so-called spring predictability barrier (Jin et al. 2008; Ren et al 2016). Another interesting aspect of the OND ATL3, which is observed before the spring, is that it can potentially contribute to ENSO prediction across the spring barrier.

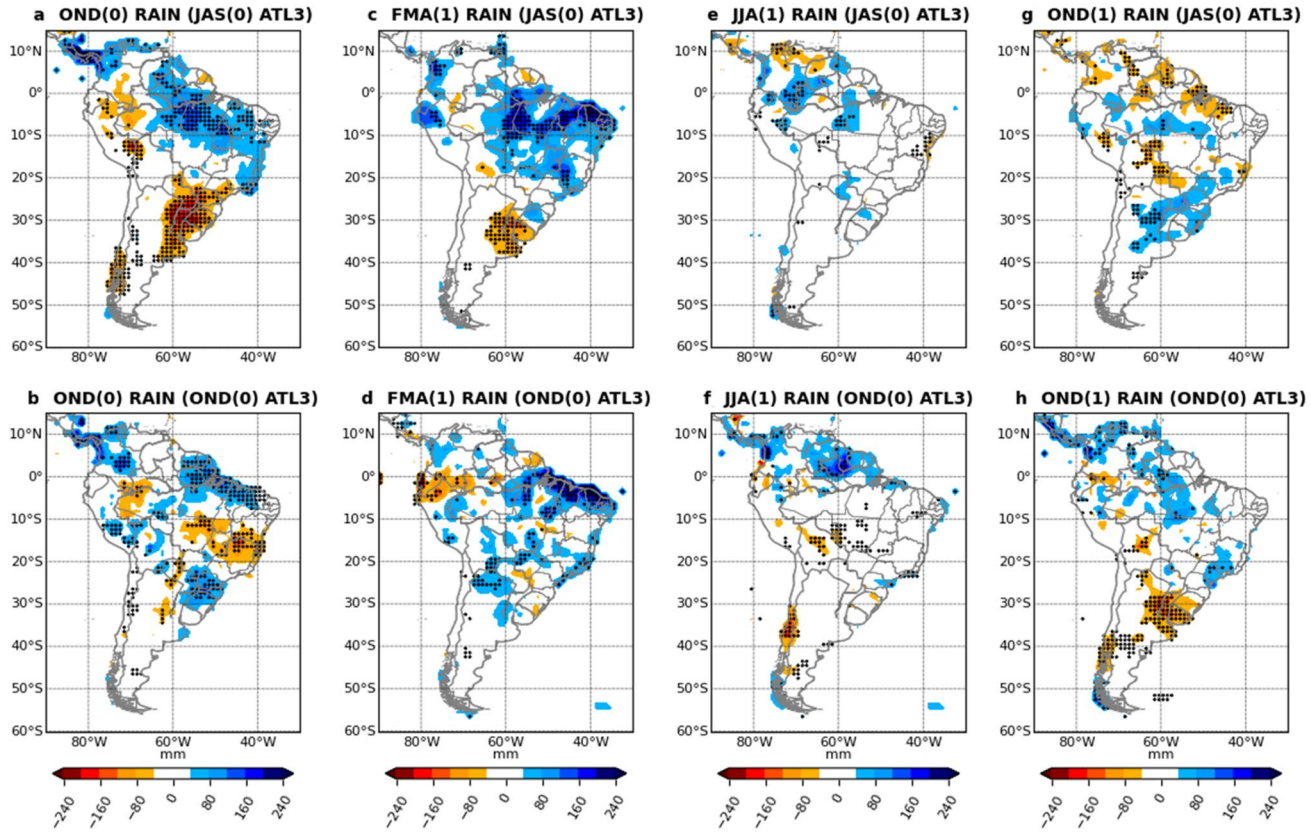

Fig. 6 Difference of composite of 3-month accumulated precipitation (shading, mm) anomalies from OND(0) to OND(1) based on: (**a**, **c**, **e** and **g**) JAS(0) ATL3 and (**b**, **d**, **f** and **h**) OND(0) ATL3. The difference is based on composite of positive ATL3 SSTA events minus composite of negative ATL3 events. Precipitations data are from GPCC for the period 1905–2014. Hatching indicate difference significant at 95% confidence level according to Welch's test

A specific analysis (not shown) of the consecutive events of the same sign, i.e. positive (negative) OND(0) ATL3 followed by positive (negative) JAS(1) ATL3 (exclude from the years used for the composites) are, in general, associated with longer duration of the associated ENSOs, which start in March(1) and end in March(2). In other words, warm (cold) winter ATL3 followed by warm (cold) summer ATL3 contribute to the same cold (warm) ENSO of long duration. Among the most recent examples are negative OND1996–JAS1997 ATL3 associated with El Niño 1997–1998 and positive OND1997–JAS1998 ATL3 associated with La Niña 1998–1999.

3.3 Implications for South American climate

In this section we analyze the impacts of the summer and winter Atlantic Niño on the South American climate variability. Figure 6 displays the difference of composites of 3-month accumulated precipitation anomalies over the South America from OND(0) to OND(1) using JAS Atlantic Niño (top panels) and OND Atlantic Niño (bottom panels).

During JAS(0) ATL3 events, positive rainfall anomalies occur over the northern part of the South America from 60° W to eastern coast in OND(0), while negative rainfall anomalies are located in the southeast South America, between 20° S and 40° S (Fig. 6a). These observations correspond to the well-known influence of the Pacific ENSO on the South American climatic variability (Grimm et al. 2000, 2003, 2009; Marengo et al. 2012; Tedeschi et al. 2012; Kayano et al. 2011, 2012). This supports the influence of ENSO on the South American precipitation, which can be accessed several months in advance knowing the summer equatorial Atlantic SST anomalies. In the following early spring [i.e. FMA(1)], positive significant values of rainfall anomalies are observed over a large part of South America, between 60° W and the eastern coast and from the equator to 10° S (Fig. 6c). The strongest anomalies of precipitation are observed in the northern Northeast Brazil. These results corroborate the predictive effect of the JAS(0) ATL3 index on the seasonal precipitations of the northern Northeast Brazil (Hounsou-Gbo et al. 2019). From JJA(1) to OND(1) (Fig. 6e, g) no strong precipitation anomalies are observed

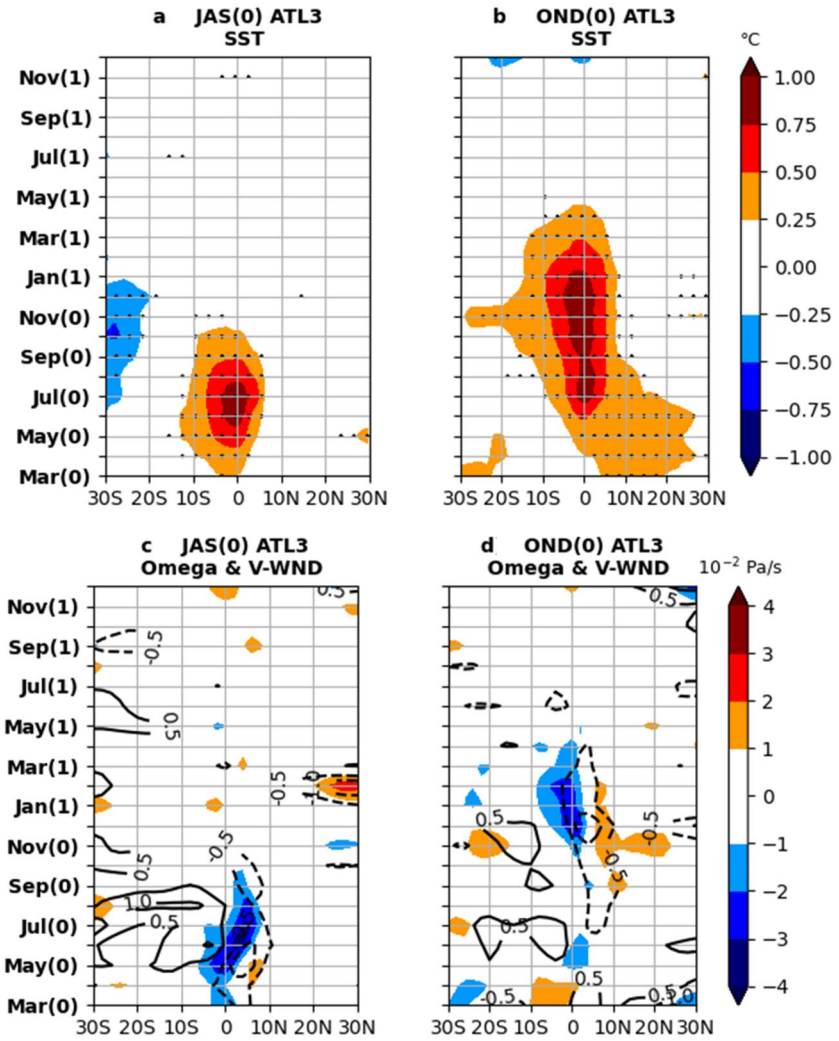

Fig. 7 Latitude-time diagram of the difference of composite of: **a**, **b** SST anomalies and **c**, **d** 500 hPa vertical velocity (shading, 10^{-2} Pa/s; negative upward) and surface meridional wind (contours, m/s; negative northerly) anomalies. Difference of composite in **a** and **c** are based on JAS(0) ATL3 events and difference of composite in **b** and **d** are based on OND(0) ATL3 events. Anomalies of SST are averaged between 45° W and 0°; anomalies of vertical velocity and meridional wind are averaged between 40°–20° W. Black dots in **a** and **b** indicate difference significant at 95% confidence level according to Welch's test for SST anomalies

over the South America, although some isolated regions of significant differences are noted.

For winter Atlantic Niño events, significant positive anomalies of precipitation are observed along the coastal strip of Northern Brazil and in the eastern central South America, between 30°–20° S (Fig. 6b). Relatively weak negative anomalies are observed between 20°–10° S in the eastern South America (Fig. 6b). During the following spring [FMA(1)], strong positive significant values of precipitation anomalies are marked along the northern coast of Northeast Brazil (Fig. 6d). Significant precipitation anomalies are also observed in the central South America and in other isolated regions. However, by contrast with the JAS(0) ATL3 event, a dipole-like of precipitation anomalies is not identified in FMA(1) over the South America (Fig. 6c vs. d). Note that the significant anomalies of precipitation observed over the northern Northeast Brazil in this case (Fig. 6d) are not related to the Pacific. Indeed, it has been shown (Fig. 4b) that the OND(0) ATL3 is not significant connected to contemporary ENSO. The tropical Atlantic plays an important role in these precipitation anomalies in northern Northeast Brazil. More details on these assumptions are given below. In JJA(1), significant positive values of precipitation anomalies are noted only over the northern South America, between the latitudes 10° N–0°, and other isolated regions (Fig. 6f). In OND(1), a dipole-like precipitation anomalies is observed with weak positive values in northern South America and significant negative values in the southeast South America (Fig. 6h). Although with smaller values, this dipole-like pattern is similar to that of OND(0) which is characteristic of the influence of ENSO (Fig. 6a vs. h). We argue that this dipole-like pattern is weaker compare to that of Fig. 6a because ENSO is in its decay phase in this case. The longer lead time between the OND(0) ATL3 and OND(1) can also be one reason for the weak signal in precipitation anomalies.

In order to identify the mechanism associated with the winter/spring precipitation over the northeast Brazil during winter Atlantic Niño events, we analyzed some selected ocean–atmosphere variables in the tropical Atlantic. In Fig. 7, we show the latitude-time diagram of the differences

of composites of the SST (averaged between the longitudes 45° W and 0°), the 500 hPa vertical velocity and the surface meridional wind anomalies (averaged between the longitudes 40° W and 20° W) corresponding to both summer (Fig. 7, left panels) and winter (Fig. 7, right panels) Atlantic Niño events.

For JAS(0) ATL3, positive significant signal of SST anomalies is observed in the south equatorial Atlantic, between 5° N and 10° S, from April(0) to October(0) (Fig. 7a). The strongest value (> 0.5 °C) is marked in summer(0) along the equator. Significant negative anomalies are noted south of 20° S in the tropical Atlantic from August(0) to December(0). The observed positive anomalies are associated with strong upward vertical velocities ($< -2\ 10^{-2}$ Pa/s) in the equatorial region from spring(0) to summer(0) (Fig. 7c). These ascending motions are related to anomalous northerly winds (i.e. negative) mainly in the north equatorial Atlantic, when the ITCZ is shifting to the north. Strong anomalous southerly winds (> 0.5 m/s) are also marked in the south tropical Atlantic from May(0) to September(0), indicating anomalously strong southeasterly winds. No significant SST, vertical velocity and meridional wind anomalies are observed in the equatorial Atlantic from November(0) to December(1). This observation supports that the winter(0)/spring(1) precipitation in the Northeast Brazil are not directly related to tropical Atlantic variability in the case of summer Atlantic Niño.

For OND(0) ATL3, significant positive SST anomalies are noted for several months in the tropical Atlantic (Fig. 7b). From March(0) to July(0), these positive SST anomalies (0.25°–0.5 °C) are transported southward from the northern tropical Atlantic. The positive SST anomalies are limited between 5° N and 15° S from September(0) to April(1) with strongest values (> 0.5 °C) located along the equator until February(1). These positive SST anomalies last until March–April(1) with values higher than 0.25 °C. Anomalous southerly winds are observed in the south tropical Atlantic in June–July(0) and in November–December(0) (Fig. 7d). In the north equatorial Atlantic, anomalous northerly surface winds (< − 0.5 m/s) extend from fall(0) to early spring(1). From winter(0) to early spring(1), strong upward velocity anomalies ($< -2.10^{-2}$ Pa/s) are located in the southern equatorial region (Fig. 7d). Therefore, the highest upward velocity anomalies are broadly located over region of anomalously warm water in the south equatorial Atlantic while northerly wind anomalies are located north of this region. This observation supports the idea that the OND(0) ATL3 SST anomalies tend to evolve into the inter-hemispheric mode of tropical Atlantic (as previously suggested by Okumura and Xie 2006). The negative phase of this inter-hemispheric mode, primarily dominated by positive SST anomalies in the south equatorial Atlantic, is associated with anomalous northerly winds, southernmost position of the ITCZ and atmospheric convection over the region of warm water in spring(1). These conditions favor positive anomalies of precipitation in the northern Northeast Brazil in spring(1) (see Fig. 6d). The inverse occurs during positive phase of the inter-hemispheric mode. Therefore, the winter ATL3 can directly influence the spring precipitation in the northern Northeast Brazil through its impact on the Atlantic ITCZ position.

4 Summary and conclusions

The Atlantic equatorial mode and the Pacific ENSO interact through an atmospheric bridge. Previous studies have shown the importance of the summer equatorial Atlantic event for forecasting the Pacific ENSO (Keenlyside et al. 2013; Martín-Rey et al. 2015). It has also been indicated that the significant inverse relationship (i.e. a warm/cold Atlantic event related to a later cold/warm Pacific event) operated mostly during the first and last decades of the last century. Therefore, these studies, which focused primarily on summer Atlantic events, did not identify significant relationship between these two equatorial basins in the mid-twentieth century (Martín-Rey et al. 2015; Lübbecke et al. 2018).

We identified here another inverse relationship between the winter Atlantic Niño [termed Atlantic Niño II by Okumura and Xie (2006)] and the Pacific ENSO, when Atlantic leads ENSO by 6-month to nearly 1-year. This relationship presents a multidecadal modulation throughout the study period. Interestingly, the highest values of the nearly 1-year lead negative relationship are marked during decades of lowest correlation between the summer Atlantic Niño and the subsequent winter Pacific ENSO. Therefore, the leading influences of the summer and winter Atlantic Niño on ENSO seem complementary at multidecadal timescales, i.e., when one is strongly negative, the other is weak, and conversely. To some extent, the Atlantic Niño in any season can influence Pacific ENSO (not shown). Nonetheless, it should be noted that only the winter Atlantic Niño is significantly negatively correlated with the Pacific ENSO during the decades of the mid-twentieth century. Our results suggest that the same mechanism of the Atlantic–Pacific Niño teleconnection operates during both summer ATL3 and winter ATL3 events. Positive/negative SST anomalies in the equatorial Atlantic affect the Walker circulation with anomalous ascending/descending branch over the Atlantic and descending/ascending branch in the central equatorial Pacific. These perturbations in the zonal atmospheric circulation drive anomalous easterly/westerly surface wind favorable for ENSO development (Keenlyside et al. 2013; Polo et al. 2015a; Losada and Rodríguez-Fonseca 2016). However, the lead time of the strongest negative correlation between the winter Atlantic Niño [in OND(0)] and the

following winter Pacific ENSO is clearly higher than that previously identified (i.e., summer ATL3 thru subsequent winter ENSO).

Our study suggests that the winter Atlantic Niño leads to an earlier development of ENSO during the following year. The early development of ENSO is associated with its mature phase in summer/fall, which tends to terminate in winter, in agreement with Wu et al. (2019). This is particularly observed when the leading teleconnection between winter ATL3 and next year development of ENSO is strongest (in the decades of the mid-twentieth century). The duration of the summer Atlantic Niño up to winter mainly in decades of the mid-twentieth century can also explain the change in the Atlantic–Pacific teleconnection at multidecadal timescale. The hindcast of the Niño3 using winter ATL3 as predictor is clearly better than that using the summer ATL3 in the decades of mid-twentieth century. We argue that the weaker ocean–atmosphere interaction in the equatorial Pacific in spring (Zebiak and Cane 1987; Blumenthal 1991) could explain the low oceanic response during this season. Indeed, when this teleconnection mechanism is initiated in the equatorial Atlantic, the Pacific ENSO is generally in transition phase (Torrence and Webster 1998). Nevertheless, more detailed studies are needed to understand the mechanisms of this delayed oceanic response in the equatorial Pacific.

Our results support that both summer and winter Atlantic Niño events could be relevant for the Pacific ENSO predictability, not only during some decades, but throughout all the 1905–2014 study period. Only the lead time between Atlantic and Pacific relationship, which depends on the active mode of Atlantic equatorial event (summer or winter), changes over the entire period. The advantage of the winter Atlantic Niño is that it could bridge the spring barrier to ENSO prediction. As noted here and also suggested by previous studies (Polo et al. 2015a; Martín-Rey et al. 2014, 2015, 2018; Lübbecke et al. 2018), the Atlantic–Pacific teleconnection is associated with variability in each basin at multidecadal timescale that can be modulated by the AMO.

It is shown that the summer Atlantic events impact the South American rainfall variability during boreal winter and spring through their teleconnection with Pacific ENSO. The winter Atlantic events also influence the variability of South America precipitation in two ways. Firstly, they affect the spring northern Northeast Brazil rainfall through their evolution into the inter-hemispheric mode of tropical Atlantic. They also affect the South American precipitation through their link to the following year's ENSO although this influence is relatively weak.

This study does not address mechanisms that control the long-term variability and duration of Atlantic equatorial modes. Recent studies have indicated that the AMO can modulate the multidecadal variability of the Atlantic equatorial mode (Martín-Rey et al. 2018). They suggested that the variability of summer SST anomalies are enhanced in the equatorial Atlantic under negative phases of the AMO. Though, there are still a number of uncertainties regarding the mechanisms that control the variability of the equatorial Atlantic from seasonal to decadal timescales. Some authors have indicated that the variance of the Atlantic Niño depends primarily on thermodynamic feedbacks rather than on the dynamic interaction between the ocean and the atmosphere (Nnamchi et al. 2015). On the other hand, other studies support the important contribution of dynamic processes to the variability of equatorial Atlantic (Jouanno et al. 2017). Meridional advection of SST anomalies from the north to the equator, reflection of Rossby waves in the western boundary, among others mechanisms, are also suggested to generate Atlantic Niño (Foltz et al. 2010; Richter et al. 2013; Lübbecke and McPhaden 2012; Lübbecke et al. 2018). Note also that, current climate model simulations present large systematic errors in tropical Atlantic mainly in the eastern equatorial Atlantic and in the Benguela region, with models' simulations warmer than observations (Richter 2015; Lübbecke et al. 2018). Accordingly, a better understanding of the mechanisms governing the Atlantic Niño variability and its inter-basin teleconnection should improve the predictability of ENSO and associated climate impacts for the future years.

Acknowledgements This study is a component of the project "Elaboração de Estudos de Suporte ao Planejamento e à Gestão de Sistemas Hídricos no Nordeste, com foco no Abastecimento Urbano e na Operação de Infraestruturas Hídricas de Uso Múltiplo" (Grant 001/2016 ANA/FUNCEME SICONV 863.189/2016). J. S. thanks FUNCEME (Edital 01/2016) for its support at Fortaleza, CE, Brazil. This work also represents collaboration by the INCT AmbTropic, the Brazilian National Institute of Science and Technology for Tropical Marine Environments, CNPq/FAPESB (grants 565054/2010-4 and 8936/2011 and 465634/2014-1) and the Brazilian Research Network on Global Climate Change FINEP/Rede CLIMA (grants 01.13.0353-00). This is a contribution to the LMI-TAPIOCA and to the TRIATLAS project, which has received funding from the European Union's Horizon 2020 research and innovation program under grant agreement No 817578. We acknowledge Met Office Hadley Centre observations datasets (https://www.metoffice.gov.uk/hadobs/) for HadISST and EN.4.2.1 dataset. The 20th Century Reanalysis V3 data are provided by the NOAA/OAR/ESRL PSD, Boulder, Colorado, USA, from their Web site at https://www.esrl.noaa.gov/psd/. GPCC Precipitation data are provided by the NOAA/OAR/ESRL PSD, Boulder, Colorado, USA, from their Web site at https://www.esrl.noaa.gov/psd/.

Compliance with ethical standards

Conflict of interest The authors declare that there is no conflict of interest regarding the publication of this paper.

References

Alexander MA, Blade I, Newman M, Lanzante JR, Lau NC, Scott JD (2002) The atmospheric bridge: the influence of ENSO

teleconnections on air-sea interaction over the global oceans. J Clim 15(16):2205–2231
An SI, Wang B (2001) Mechanisms of locking of the El Niño and La Niña nature phases to boreal winter. J Clim 14:2164–2176
Ashok K, Behera S, Rao AS, Weng H, Yamagata T (2007) El Niño Modoki and its teleconnection. J Geophys Res 112:C11007. https://doi.org/10.1029/2006JC003798
Bjerknes J (1969) Atmospheric teleconnections from the equatorial Pacific. Mon Wea Rev 97:163–172
Blumenthal MB (1991) Predictability of a coupled atmosphere-ocean model. J Clim 4:766–784
Cai W et al (2019) Pantropical climate interactions. Science. https://doi.org/10.1126/science.aav4236
Cane MA (2005) The evolution of El Niño, past and future. Earth Planet Sci Lett 230:227–240
Caniaux G, Giordani H, Redelsperger J-L, Guichard F, Key E, Wade M (2011) Coupling between the Atlantic cold tongue and the West African monsoon in boreal spring and summer. J Geophys Res. https://doi.org/10.1029/2010JC00657
Chang P, Fang Y, Saravanan R, Ji L, Seidel H (2006) The cause of the fragile relationship between the Pacific El Ninño and the Atlantic Niño. Nature 443:324–328. https://doi.org/10.1038/nature05053
Chiang JC, Kushnir Y, Zebiak SE (2000) Interdecadal changes in eastern Pacific ITCZ variability and its influence on the Atlantic ITCZ. Geo Res Lett 27:3687–3690
Compo GP, Whitaker JS, Sardeshmukh PD et al (2011) The twentieth century reanalysis project. Q J R Meteor Soc 137:1–28
Delécluse P, Servain J, Levy C, Arpe K, Bengtsson L (1994) On the teleconnection between the 1984 Atlantic warm event and the 1982–1983 ENSO. Tellus 46A:448–464
Ding H, Keenlyside N, Latif M (2009) Seasonal cycle in the upper equatorial Atlantic Ocean. J Geophys Res 114(C9):C09016
Ding H, Keenlyside NS, Latif M (2012) Impact of the equatorial Atlantic on the El Nino southern oscillation. Clim Dyn 38:1965–1972. https://doi.org/10.1007/s00382-011-1097-y
Dong BW, Sutton RT, Scaife AA (2006) Multidecadal modulation of El Nino-Southern oscillation (ENSO) variance by Atlantic Ocean sea surface temperatures. Geophys Res Lett. https://doi.org/10.1029/2006GL025766
Enfield DB, Mayer DA (1997) Tropical Atlantic sea surface temperature variability and its relation to El Niño-Southern Oscillation. J Geophys Res 102:929–945
Foltz GR, McPhaden MJ (2010) Abrupt equatorial wave-induced cooling of the Atlantic cold tongue in 2009. Geophys Res Lett 37:L24605. https://doi.org/10.1029/2010GL045522
Frauen C, Dommenget D (2012) Influences of the tropical Indian and Atlantic Oceans on the predictability of ENSO. Geophys Res Lett 39:L02706. https://doi.org/10.1029/2011GL050520
Giannini A, Chiang JCH, Cane MA, Kushnir Y, Seager R (2001) The ENSO teleconnection to the tropical Atlantic Ocean: contributions of the remote and local SSTs to rainfall variability in the tropical Americas. J Clim 14:4530–4544
Giannini A, Saravanan R, Chang P (2004) The preconditioning role of tropical Atlantic variability in the development of the ENSO teleconnection: implications for the prediction of Nordeste rainfall. Clim Dyn 22:839–855
Giese BS, Seidel HF, Compo GP, Sardeshmukh PD (2016) An ensemble of ocean reanalyses for 1815–2013 with sparse observational input. J Geophys Res Oceans 121:6891–6910. https://doi.org/10.1002/2016JC012079
Grimm AM (2003) The El Niño impact on the summer monsoon in Brazil: regional processes versus remote influences. J Clim 16:263–280
Grimm AM, Tedeschi RG (2009) ENSO and extreme rainfall events in South America. J Clim 22:1589–1609
Grimm AM, Barros VR, Doyle ME (2000) Climate variability in southern South America associated with El Niño and La Nina events. J Clim 13:35–58
Ham YG, Kug JS, Park JY, Jin FF (2013) Sea surface temperature in the north tropical Atlantic as a trigger for El Niño/Southern oscillation events. Nat Geosci 6:112–116
Hounsou-Gbo GA, Servain J, Araujo M, Caniaux G, Bourlès B, Fontenele D, Martins ESPR (2019) SST indexes in the Tropical South Atlantic for forecasting rainy seasons in northeast Brazil. Atmosphere 10:335
Izumo T, Vialard J, Lengaigne M, de Boyer MC, Behera SK, Luo J-J (2010) Influence of the state of the Indian Ocean dipole on the following year's El Niño. Nat Publ Group 3(3):168–172
Jia F, Cai WJ, Wu LX, Gan BL, Wang GJ, Kucharski F, Chang P, Keenlyside N (2019) Weakening Atlantic Niño-Pacific connection under greenhouse warming. Sci Adv 5(8):4111. https://doi.org/10.1126/sciadv.aax4111
Jin EK et al (2008) Current status of ENSO prediction skill in coupled ocean-atmosphere models. Clim Dyn 31:647–664. https://doi.org/10.1007/s00382-008-0397-3
Jouanno J, Hernandez O, Sanchez-Gomez E (2017) Equatorial Atlantic interannual variability and its relation to dynamic and thermodynamic processes. Earth Syst Dyn 8:1061–1069
Kayano MT, Andreoli RV (2006) Relationship between rainfall anomalies over northeastern Brazil and the El Niño-Southern Oscillation. J Geophys Res 111(D13):101
Kayano MT, Valéria Andreoli R, Ferreira de Souza RA (2011) Evolving anomalous SST patterns leading to ENSO extremes: relations between the tropical Pacific and Atlantic Oceans and the influence on the South American rainfall. Int J Climatol 31:1119–1134. https://doi.org/10.1002/joc.2135
Kayano MT, Andreoli RV, Ferreira de Souza RA (2012) Relations between ENSO and the South Atlantic SST modes and their effects on the South American rainfall. Int J Climatol 33(8):2008–2023. https://doi.org/10.1002/joc.3569
Keenlyside NS, Latif M (2007) Understanding equatorial Atlantic interannual variability. J Clim 20:131–142
Keenlyside NS, Ding H, Latif M (2013) Potential of equatorial Atlantic variability to enhance El Nino prediction. Geophys Res Lett 40:2278–2283. https://doi.org/10.1002/grl.50362
L'Heureux ML, Takahashi K, Watkins AB, Barnston AG, Becker EJ, Di Liberto TE, Gamble F, Gottschalck J, Halpert MS, Huang B, Mosquera-Vásquez K, Wittenberg AT (2017) Observing and predicting the 2015–2016 El Niño. Bull Am Meteorol Soc. https://doi.org/10.1175/BAMS-D-16-0009.1
Latif M, Barnett TP (1995) Interactions of the Tropical Oceans. J Clim 8:952–964
Losada T, Rodríguez-Fonseca B (2016) Tropical atmospheric response to decadal changes in the Atlantic equatorial mode. Clim Dyn 47:1211–1224. https://doi.org/10.1007/s00382-015-2897-2
Lübbecke JF, McPhaden MJ (2012) On the inconsistent relationship between Pacific and Atlantic Niños. J Clim 25:4294–4303. https://doi.org/10.1175/JCLI-D-11-00553.1
Lübbecke JF, McPhaden MJ (2017) Symmetry of the Atlantic Niño mode. Geophys Res Lett 44(2):965–973. https://doi.org/10.1002/2016GL071829
Lübbecke JF, Böning CW, Keenlyside NS, Xie S-P (2010) On the connection between Benguela and equatorial Nñios and the role of the South Atlantic anticyclone. J Geophys Res. https://doi.org/10.1029/2009JC005964
Lübbecke JF, Rodríguez-Fonseca B, Richter I, Martín-Rey M, Losada T, Polo I, Keenlyside NS (2018) Equatorial Atlantic variability—modes, mechanisms, and global teleconnections. Wiley Interdiscip Rev Climate Change 9(4):1–18. https://doi.org/10.1002/wcc.527

Lutz K, Rathmann J, Jacobeit J (2013) Classification of warm and cold water events in the eastern tropical Atlantic Ocean. Atmos Sci Lett 14:102–106

Marengo JA, Liebmann B, Grimm AM et al (2012) Recent developments on the South American monsoon system. Int J Climatol. https://doi.org/10.1002/joc.2254

Marin F, Caniaux G, Bourles B, Giordani H, Gouriou Y, Key E (2009) Why were sea surface temperatures so different in the eastern equatorial Atlantic in June 2005 and 2006? J Phys Oceanogr 39:1416–1431. https://doi.org/10.1175/2008jpo4030.1

Martín-Rey M, Rodríguez-Fonseca B, Polo I, Kucharski F (2014) On the Atlantic–Pacific Niños connection: a multidecadal modulated mode. Clim Dyn 43:3163–3178

Martín-Rey M, Rodríguez-Fonseca B, Polo I (2015) Atlantic opportunities for ENSO prediction. Geophys Res Lett 42:6802–6810

Martín-Rey M, Polo I, Rodriguez-Fonseca B, Losada T, Lazar A (2018) Is there evidence of changes in Tropical Atlantic variability modes under AMO phases in the observational record? J Clim 31:515–536. https://doi.org/10.1175/JCLI-D-16-0459.1

McPhaden MJ (2003) Tropical Pacific Ocean heat content variations and ENSO persistence barriers. Geophys Res Lett 30:1480. https://doi.org/10.1029/2003GL016872

McPhaden MJ, Zhang X (2009) Asymmetry in zonal phase propagation of ENSO sea surface temperature anomalies. Geophys Res Lett 36:L13703

Merle J (1983) Seasonal variability of subsurface thermal structure in the Tropical Atlantic Ocean. Elsevier Oceanogr Ser 36:31–49. https://doi.org/10.1016/s0422-9894(08)70626-3

Merle J, Fieux M, Hisard P (1980) Annual signal and interannual anomalies of sea surface temperature in the eastern equatorial Atlantic Ocean. Deep-Sea Res 26:77–101

Nnamchi HC, Li J, Kucharski F, Kang IS, Keenlyside NS, Chang P, Farneti R (2015) Thermodynamic controls of the Atlantic Niño. Nat Commun 6:8895. https://doi.org/10.1038/ncomms9895

Nobre P, Shukla J (1996) Variations of sea surface temperature, wind stress, and rainfall over the tropical Atlantic and South America. J Clim 9:2464–2479

Okumura YM, Deser C (2010) Asymmetry in the duration of El Nino and La Nina. J Clim 23:5826–5843

Okumura Y, Xie S-P (2006) Some overlooked features of tropical Atlantic climate leading to a new Nino-like phenomenon. J Clim 19:5859–5874

Park JH, Li T (2019) Interdecadal modulation of El Niño–tropical North Atlantic teleconnection by the Atlantic multi-decadal oscillation. Clim Dyn 52:5345–5360. https://doi.org/10.1007/s00382-018-4452-4

Picaut J (1983) Propagation of seasonal coastal upwelling in the eastern equatorial Atlantic. J Phys Oceanogr 13:18–37

Polo I, Lazar A, Rodriguez-Fonseca B, Mignot J (2015b) Growth and decay of the equatorial Atlantic SST mode by means of closed heat budget in a coupled general circulation model. Front Earth Sci 3:37. https://doi.org/10.3389/feart.2015.00037

Polo I, Martin-Rey M, Rodriguez-Fonseca B, Kucharski F, Mechoso CR (2015a) Processes in the Pacific La Nina onset triggered by the Atlantic Nino. Clim Dyn 44:115–131. https://doi.org/10.1007/s00382-014-2354-7

Rayner NA, Parker DE, Horton EB, Folland CK, Alexander LV, Rowell DP, Kent EC, Kaplan A (2003) Global analyses of sea surface temperature, sea ice, and night marine air temperature since the late nineteenth century. J Geophys Res Atm 108(D14):4407. https://doi.org/10.1029/2002JD002670

Ren H-L, Jin F-F, Tian B et al (2016) Distinct persistence barriers in two types of ENSO. Geophys Res Lett 43:10973–10979

Richter I (2015) Climate model biases in the eastern tropical oceans: causes, impacts and ways forward. WIRE Clim Change 6:345–358. https://doi.org/10.1002/wcc.338

Richter I, Behera SK, Masumoto Y, Taguchi B, Sasaki H, Yamagata T (2013) Multiple causes of interannual sea surface temperature variability in the equatorial Atlantic Ocean. Nat Geosci 6(1):43–47. https://doi.org/10.1038/Ngeo1660

Rodrigues RR, McPhaden MJ (2014) Why did the 2011–2012 La Niña cause a severe drought in the Brazilian Northeast? Geophys Res Lett 41:1012–1018. https://doi.org/10.1002/2013GL058703

Rodrigues RR, Campos EJD, Haarsma R (2015) The impact of ENSO on the South Atlantic subtropical dipole mode. J Clim 28(7):2691–2705. https://doi.org/10.1175/JCLI-D-14-00483.1

Rodriguez-Fonseca B, Polo I, Garcia-Serrano J, Losada T, Mohino E, Mechoso CR, Kucharski F (2009) Are Atlantic Ninos enhancing Pacific ENSO events in recent decades? Geophys Res Lett 36:L20705. https://doi.org/10.1029/2009GL040048

Santoso A, Mcphaden MJ, Cai W (2017) The defining characteristics of ENSO extremes and the strong 2015/2016 El Niño: ENSO extremes. Rev Geophys 55(4):1079–1129. https://doi.org/10.1002/2017RG000560

Schneider U, Becker A, Finger P, Meyer-Christoffer A, Ziese M, Rudolf B (2013) GPCC's new land surface precipitation climatology based on quality-controlled in situ data and its role in quantifying the global water cycle. Theor Appl Climatol 115:15–40

Servain J, Picaut J, Merle J (1982) Evidence of remote forcing in the equatorial Atlantic Ocean. J Phys Oceanogr 12:457–463

Servain J, Busalacchi A, McPhaden M, Moura A-D, Reverdin G, Vianna M, Zebiak S (1998) A pilot research moored array in the tropical Atlantic (PIRATA). Bull Am Meteor Soc 79:2019–2031

Servain J, Wainer I, McCreary JP, Dessier A (1999) Relationship between the equatorial and meridional modes of climatic variability in the tropical Atlantic. Geophys Res Lett 26:485–488

Tedeschi RG, Cavalcanti IFA, Grimm AM (2012) Influences of two types of ENSO on South American precipitation. Int J Climatol 33:1382–1400

Tokinaga H, Richter I, Kosaka Y (2019) ENSO influence on the Atlantic Niño, revisited: Multi-year versus single-year ENSO events. J Clim 32:4585–4600

Torrence C, Webster PJ (1998) The annual cycle of persistence in the El Niño/Southern Oscillation. Q J R Meteor Soc 124:1985–2004

Trenberth KE (1997) The definition of El Niño. Bull Am Meteor Soc 78:2771–2777

Uvo CB, Repelli CA, Zebiak SE, Kushnir Y (1998) The relationship between tropical Pacific and Atlantic SST and northeast Brazil monthly precipitation. J Clim 11:551–562

Wang C (2019) Three-ocean interactions and climate variability: a review and perspective. Clim Dyn 53:5119–5136. https://doi.org/10.1007/s00382-019-04930-x

Wauthy B (1983) Introduction à la climatologie du Golfe de Guinée. Océanogr Trop 18(2):103–138

Wolter K, Timlin MS (1998) Measuring the strength of ENSO events—how does 1997/98 rank? Weather 53:315–324. https://doi.org/10.1002/j.1477-8696.1998.tb06408.x

Wu X, Okumura YM, DiNezio PN (2019) What controls the duration of El Niño and La Niña events? J Climate 32:5941–5965. https://doi.org/10.1175/JCLID-18-0681.1

Yu J-Y, Lau KM (2005) Contrasting Indian Ocean SST variability with and without ENSO influence: a coupled atmosphere-ocean GCM study. Meteorol Atmos Phys 90:179–191. https://doi.org/10.1007/s00703-004-0094-7

Zebiak SE (1993) Air–sea interaction in the equatorial Atlantic region. J Clim 6:1567–1586

Zebiak SE, Cane MA (1987) A model El Niño Southern Oscillation. Mon Wea Rev 115:2262–2278